

Multi-resolution Texture Classification Based on Local Image Orientation

Ovidiu Ghita, Paul F. Whelan, and Dana E. Ilea

Vision Systems Group,
Dublin City University, Dublin 9, Ireland
{ghitao,whelanp,danailea}@eeng.dcu.ie
<http://www.eeng.dcu.ie/~vsl>

Abstract. The aim of this paper is to evaluate quantitatively the discriminative power of the image orientation in the texture classification process. In this regard, we have evaluated the performance of two texture classification schemes where the image orientation is extracted using the partial derivatives of the Gaussian function. Since the texture descriptors are dependent on the observation scale, in this study the main emphasis is placed on the implementation of multi-resolution texture analysis schemes. The experimental results were obtained when the analysed texture descriptors were applied to standard texture databases.

Key words: Local image orientation, texture classification, SVM, multi-resolution.

1 Introduction

Texture is a fundamental property that has been widely applied to partition digital images into regions that are homogenous with respect to some structural measures. This approach is motivated by the fact that the objects that are present in digital images are not described only by their shapes but also by the structural relationship between the pixels in the image. While there is not a widely accepted definition for texture within the computer vision community, most of the developed techniques approach the texture analysis either from a structural or a statistical perspective [5],[9],[12],[13]. In statistical approaches, the texture is described by the spatial distribution of the pixels in the image [3] while in structural approaches the texture is defined as a relational arrangement of texture primitives [14],[18].

In this paper our aim is to evaluate two texture extraction techniques that sample the image orientation at micro and macro levels. The texture analysis techniques followed in this paper evaluate the global distributions of the local image orientations that are calculated for each pixel in the image in a predefined neighbourhood. In this paper we extracted the global image orientation using the distribution of the edge orientation (EO) [10] and the Scale-Orientation Histogram (SOH) that were developed for image retrieval [19]. The local orientation features are measures that sample how strongly the texture is oriented along

one direction and they are generally calculated at a particular observation scale [6],[8],[15]. While the texture orientation is sensitive to the observation scale, in this study one of our major goals is to evaluate the discriminative power of the orientation distributions when calculated at different resolutions. In our study, to further enhance the discriminative power of the texture orientation distribution, some contrast measures were included in the construction of the local texture descriptors.

This paper is organized as follows. Section 2 describes the mathematical background behind the calculation of the edge orientation while Section 3 details the Scale Orientation Histogram (SOH) texture extraction method. Section 4 presents the implementation of the texture classification framework. Section 5 describes the experimental results while in Section 6 are provided concluding remarks.

2 Estimation of Edge Orientation

The local orientation in the image I is typically obtained by calculating the first derivatives in two orthogonal directions [11] as follows,

$$\nabla I = \left[\frac{\partial I}{\partial x}, \frac{\partial I}{\partial y} \right] = [I_x, I_y], \quad \Theta = \arctan \left(\frac{\partial I / \partial y}{\partial I / \partial x} \right) \quad (1)$$

where ∇ defines the gradient operator and Θ is the edge orientation. To circumvent the problems caused by the image noise, we have calculated the partial derivatives in the x and y directions with filters that implement the derivatives of the Gaussian function. This is achieved by filtering the image with 1-dimensional (1D) operators that are calculated using the expression illustrated in equation 2.

$$G(x) = \frac{1}{\sqrt{2\pi}\sigma} e^{-\frac{x^2}{2\sigma^2}}, \quad \frac{\partial G}{\partial x} = -\frac{x}{\sigma^2} G(x) \quad (2)$$

where σ is the scale of the Gaussian function. The main advantage of the calculation of the partial derivatives using the derivative of the Gaussian resides in the fact that the Gaussian has a smoothing effect and the scale parameter σ controls the amount of noise reduction. After the calculation of the partial derivatives, the weak edge responses were eliminated by applying a non-maxima suppression procedure (similar to that described in [2]) and the edge orientation is determined at micro level for each pixel in the image using the expression illustrated in equation 1. The texture orientation can be estimated at macro-level by the distribution of edge orientations that is calculated over the entire image. The calculation of the macro-texture distributions will be addressed in the next section.

2.1 Estimation of the Dominant Orientation of Texture at Micro and Macro-level

The problem of analysing the texture orientation at a given observation scale is not a straightforward task as the orientation of the texture may be isotropic at macro level but having strong orientation at micro-level. This issue has been initially addressed in the paper by Germain et al. [7] and later in the paper by Ilea et al. [10]. In this paper, we estimate the orientation of the texture at micro level by constructing the histogram of orientations for all pixels in the local neighbourhood Ω and the dominant orientation is selected as the dominant peak in the histogram as follows,

$$H_{\Theta} = \bigcup_{p \in D} h_{\Theta}(p), \quad h_{\Theta}(p) = \int_{\Omega} \delta(\Theta(i, j), p) d\Omega, \quad (3)$$

$$\text{where } (i, j) \in \Omega, \quad D \in [0, 2\pi], \quad \delta(u, v) = \begin{cases} 1 & u = v \\ 0 & u \neq v \end{cases} \quad (4)$$

$$\Theta_d = \text{argmax}(H_{\Theta}) \quad (5)$$

where Θ is the local orientation, p is the orientation bin, D defines the orientation domain, H_{Θ} is the distribution of local orientations and Θ_d is the dominant orientation of the texture in the neighbourhood Ω . The dominant orientation calculated at macro-level (H_{Θ_d}) is simply estimated by the distribution of the dominant orientations that are calculated over the entire image (see equation 6).

$$H_{\Theta_d} = \bigcup_{p \in D} \int_{\Gamma} \delta(\Theta_d^{\Omega}(i, j), p) d\Gamma \quad (6)$$

where Γ is the image domain. In equation (6) it should be noted that the texture orientation is sampled at a predefined observation scale that is controlled by the size of the local neighbourhood Ω .

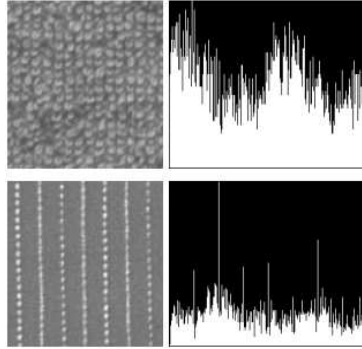


Fig. 1. Distributions of edge orientation calculated for two textures (top - isotropic and bottom - oriented) from the Outex database [17].

3 Scale Orientation Histogram

In the estimation of the Scale Orientation Histogram (SOH), the orientation for each pixel in the image is calculated in a predefined neighborhood Ω using an expression that is derived from (1) as follows [11],[19],

$$\Theta_{\Omega}(i, j) = \frac{1}{2} \arctan \left(\frac{\int_{\Omega} 2I_x(i, j)I_y(i, j)d\Omega}{\int_{\Omega} (I_x^2(i, j) - I_y^2(i, j)) d\Omega} \right) + \frac{\pi}{2} \quad (7)$$

where $(i, j) \in \Omega$ are the pixel coordinates and I_x and I_y are the partial derivatives calculated in the x and y directions. To calculate the SOH we need to determine an additional measure (that is referred in Zhou et al. [19] to as anisotropic strength) using the following expression,

$$g_{\Omega}(i, j) = \frac{[\int_{\Omega} (I_x^2(i, j) - I_y^2(i, j)) d\Omega]^2 + [\int_{\Omega} 2I_x^2(i, j)I_y^2(i, j)d\Omega]^2}{[\int_{\Omega} (I_x^2(i, j) + I_y^2(i, j)) d\Omega]^2} \quad (8)$$

Note that in equations (7) and (8) the orientation and anisotropic strength measures are calculated within the neighborhood Ω that is related to the observation scale where the texture is analysed. From equation (8) it can be observed that the anisotropic strength approaches the value 1.0 when the texture is oriented and it has a value close to zero when the texture has isotropic characteristics. The SOH is constructed by mapping the image intensity domain Γ into a two dimensional (2D) representation as follows,

$$SOH(\Omega, \alpha) = \sum_{(i, j) \in \Gamma} \{g_{\Omega}(i, j) \mid \Theta_{\Omega}(i, j) = \alpha\} \quad (9)$$

where the local neighborhood can take values in the interval $\Omega \in [1, \Gamma]$ and $\alpha \in [0, \pi]$. The main advantage of the SOH is that by varying the scale observation parameter Ω , we can construct a compact 2D representation of the image where the orientation of the texture is sampled at different resolutions or observation scales.

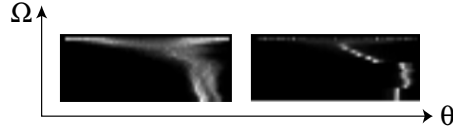


Fig. 2. Example showing the SOH measures calculated for texture images illustrated in Fig. 1. (Left) Isotropic texture. (Right) Oriented texture. For clarity purposes the parameter Ω was varied in the interval $[1, 20]$ and the orientation Θ has been re-sampled to 64 bins.

4 Construction of Texture Feature Vectors

The dominant orientation in the image is a powerful local texture descriptor, but it is worth noting that it is not robust in sampling the difference between textures that are subjected to illumination variation and image inversion. To address this issue, the local texture orientation (H_{Θ_d}) is augmented with measures such as contrast and local orientation coherence that are calculated in the local neighbourhood Ω (where the dominant orientation of the texture has been estimated). As indicated in Ilea et al. [10], the contrast measure is sampled by the mean gray-scale value calculated in the neighbourhood Ω and the orientation coherence (Θ_c) is calculated using the weighted standard deviation of the edge orientation of all pixels in the neighbourhood as follows,

$$\Theta_c(i, j) = \sqrt{\frac{1}{k^2} \sum_{m, n \in w_{k \times k}(\Omega)} (I_x^2(m, n) + I_y^2(m, n)) (\Theta(m, n) - \Theta_{ave})^2} \quad (10)$$

where (i, j) are the coordinates of the pixel of interest, I_x and I_y are the partial derivatives calculated for all pixels with coordinates (m, n) in the window $w_{k \times k} = \Omega$ and Θ_{ave} is the average edge orientation calculated for all pixels in the window $w_{k \times k}$. The feature vector for the edge orientation (EO) technique is formed by the three distributions, namely the dominant orientation, the contrast and the orientation coherence that are calculated over the entire image at different orientation scales (the orientation scales are varied in small increments to sample the oriented or isotropic characteristics of the texture).

When analysing the texture orientation using the SOH method the feature vector is defined by the SOH distribution that is calculated for a predefined number of observation scales (see equation 9) and this distribution is augmented by the contrast measure that is calculated as the distribution of the mean-gray values calculated in the neighbourhood Ω .

5 Experiments and Results

The experimental results reported in this paper were conducted on Outex (TC 00000 and TC 00001) databases and on databases that were constructed by recursively splitting the images contained in the Brodatz database [1]. The Outex databases [17] are formed by 24 classes of standard textures (canvas, carpet and tile) and they are depicted in Fig. 3.

The database TC 00000 consists of 480 texture images where the image size is 128×128 . Database TC 00001 comprises 2212 texture images where the image size is 64×64 . The Brodatz database used in our study consists of a set of 36 texture images. This database is formed by various oriented and isotropic textures and the original images were split in 4 (database BD 00000), 16 (database BD 00001) and 64 sub-images (database BD 00002). Database BD 00000 consists of

144 texture images (image size: 256×256), database BD 00001 has 576 texture images (image size: 128×128) and database BD 00002 comprises 2304 images (image size: 64×64). A number of Brodatz textures used in our experiments are depicted in Fig. 4.

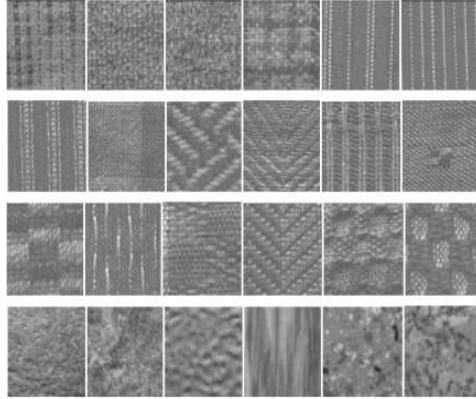


Fig. 3. The 24 textures contained in the Outex database [17].

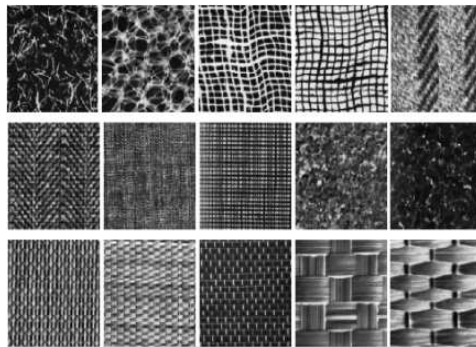


Fig. 4. Samples of the Brodatz [1] textures used in our experiments.

In our experiments we have used half of the images contained in each database for training while the remaining images were used for testing. The similarity between the training and test textures is evaluated using the SVM classification scheme [4]. In our experiments a number of tests were carried out to evaluate the influence of the scale parameter of the derivative of Gaussian operators. The experimental results indicated that the best results were obtained when the scale parameter was set to small values in the range $[0.5, 1]$. In our implementation, the scale parameter σ of the derivative of Gaussian operators was set to 0.5 to minimise the windowing effects caused by the convolution with large kernels. The next experimental tests were conducted to evaluate the effect of the observation scale on the classification results.

Table 1. The effect of the window size on the classification results.

| Database | Winsow size Ω | EO Accuracy [%] | SOH Accuracy [%] |
|--------------------|-------------------------|--------------------|---------------------|
| TC 00000 (128×128) | 3×3 | 97.08 | 81.25 |
| | 7×7 | 95.00 | 70.41 |
| | 11×11 | 84.16 | 59.58 |
| TC 00001 (64×64) | 3×3 | 95.54 | 68.75 |
| | 7×7 | 87.50 | 62.78 |
| | 11×11 | 78.21 | 49.90 |
| BD 00000 (256×56) | 3×3 | 97.22 | 98.61 |
| | 7×7 | 91.66 | 86.11 |
| | 11×11 | 84.72 | 80.55 |
| BD 00001 (128×128) | 3×3 | 99.30 | 96.52 |
| | 7×7 | 94.44 | 87.50 |
| | 11×11 | 93.75 | 76.04 |
| BD 00002 (64×64) | 3×3 | 94.96 | 84.04 |
| | 7×7 | 88.11 | 78.14 |
| | 11×11 | 85.51 | 70.94 |

The classification results depicted in Table 1 indicate that the performance of the edge orientation texture descriptors is higher than that offered by the texture analysis techniques based on the SOH distributions. Also we note that for both techniques the increase in the observation scale lowers the classification results. This is motivated by the fact that the texture descriptors calculated at low observation scales capture the local orientation properties of the texture, while with the increase in the observation scale the texture units sample better the isotropic character of the texture. This observation is very important as this opens the possibility to develop texture descriptors that sample the orientation-isotropy properties of the image by varying the observation scale in small increments.

To this end, the next experiment was conducted in order to evaluate the discriminative power of the developed texture descriptors when they are implemented in multi-resolution forms. The classification results obtained when the developed texture analysis techniques were applied to Outex and Brodatz databases are depicted in Table 2. The results shown in Table 2 demonstrate that the classification accuracy has substantially increased when the texture descriptors were implemented in multi-resolution forms (see the results obtained for the texture analysis scheme based on SOH). The classification results depicted in Table 2 indicate that the benefit of using multi-resolution operators become obvious especially when they are applied to the classification of image databases that are formed by small images (see the classification results obtained for databases TC 00001 and BD 00002). To limit the space of Table 2 we have presented the classification results when the texture is analysed at up to four observation scales. An extensive set of classification results obtained for large combinations of observation scales are available at the following web address: <http://www.eeng.dcu.ie/~vsg/code/ICLAR2008-Results.pdf>.

Table 2. Multi-resolution classification results.

| Database | Winsow size | EO Accuracy | SOH Accuracy |
|--------------------|---|-------------|--------------|
| | Ω | [%] | [%] |
| TC 00000 (128×128) | $(3 \times 3) + (5 \times 5)$ | 99.16 | 93.75 |
| | $(3 \times 3) + (5 \times 5) + (7 \times 7)$ | 99.16 | 92.08 |
| | $(3 \times 3) + (5 \times 5) + (7 \times 7) + (9 \times 9)$ | 97.91 | 90.41 |
| TC 00001 (64×64) | $(3 \times 3) + (5 \times 5)$ | 96.11 | 80.20 |
| | $(3 \times 3) + (5 \times 5) + (7 \times 7)$ | 95.54 | 82.19 |
| | $(3 \times 3) + (5 \times 5) + (7 \times 7) + (9 \times 9)$ | 94.22 | 81.06 |
| BD 00000 (256×56) | $(3 \times 3) + (5 \times 5)$ | 100 | 97.22 |
| | $(3 \times 3) + (5 \times 5) + (7 \times 7)$ | 100 | 95.83 |
| | $(3 \times 3) + (5 \times 5) + (7 \times 7) + (9 \times 9)$ | 100 | 88.88 |
| BD 00001 (128×128) | $(3 \times 3) + (5 \times 5)$ | 100 | 96.87 |
| | $(3 \times 3) + (5 \times 5) + (7 \times 7)$ | 99.65 | 94.79 |
| | $(3 \times 3) + (5 \times 5) + (7 \times 7) + (9 \times 9)$ | 99.65 | 95.13 |
| BD 00002 (64×64) | $(3 \times 3) + (5 \times 5)$ | 95.05 | 88.46 |
| | $(3 \times 3) + (5 \times 5) + (7 \times 7)$ | 94.62 | 88.98 |
| | $(3 \times 3) + (5 \times 5) + (7 \times 7) + (9 \times 9)$ | 94.27 | 88.55 |

The results depicted in Tables 1 and 2 allow us to draw some additional useful conclusions. The main important finding is that the distributions of image orientation calculated at micro-level are appropriate to describe the global and local properties of the texture. Another important finding is that the inclusion of the observation scale in a multi-resolution representation allows the development of a texture unit that is able to characterise in detail the orientation-anisotropy properties of the texture. One important advantage of the proposed texture units over other implementations such as Local Binary Patterns [16] and grayscale co-occurrence matrices [5],[9] is that the orientation distributions evaluated in this paper are π -periodic and they can be easily extended to encompass the rotational invariance.

6 Conclusions

The aim of this paper was to evaluate the discriminative power of the local image orientation in the process of texture classification. In this paper we have analysed two texture analysis techniques where the image orientation was evaluated at macro-level by the distributions of the texture units that are calculated at micro-level. The main contribution of this paper resides in the evaluation of the texture orientation at different observation scales and the experimental results indicate that the multi-resolution distributions are efficient descriptors to capture the orientation-anisotropy properties of the texture. In our future studies we will further extend these texture descriptors in order to produce a texture representation that is robust to illumination conditions and perspective

distortions. Due to their compact representation and high discriminative power, the texture descriptors analysed in this paper can be successfully included in the development of applications ranging from image segmentation to image retrieval.

Acknowledgments. This work was funded in part by the Science Foundation Ireland (Research Frontiers Programme) and the OVPR-DCU Research Fellowship Programme.

References

1. Brodatz, P.: Textures: A Photographic Album for Artists and Designers, Dover Publications, New York (1966).
2. Canny, J.: A computational approach to edge detection, *IEEE Transactions on Pattern Analysis and Machine Intelligence* **8(6)**, (1986) 679–698.
3. Chellappa, R., Kashyap, R.L., Manjunath, B.S.: Model based texture segmentation and classification, in *The Handbook of Pattern Recognition and Computer Vision*, C.H. Chen, L.F. Pau and P.S.P Wang (Editors) World Scientific Publishing (1998).
4. Chan, C., Lin, C.J.: LIBSVM: A library for support vector machines, www.csie.ntu.edu.tw/~cjlin/libsvm (2001).
5. Dyer, C.R., Hong, T., Rosenfeld, A.: Texture classification using gray level co-occurrence based on edge maxima, *IEEE Transactions on Systems, Man, and Cybernetics* **10**, (1980) 158–163.
6. Flores, M.A., Leon, L.A.: Texture classification through multiscale orientation histogram analysis, in *Scale Space Methods in Computer Vision*, LNCS **2695**, (2003) 479–493.
7. Germain, C., Da Costa, J.P., Laviolle, O., Baylou, P.: Multiscale estimation of vector field anisotropy application to texture characterization, *Signal Processing* **83**, (2003) 1487–1503.
8. Guérin-Dugué, A., Oliva, A.: Classification of scene photographs from local orientation features, *Pattern Recognition Letters* **21**, (2000) 1135–1140.
9. Haralick, R.M.: Statistical and structural approaches to texture, in *Proc of IEEE*, **67**, (1979) 786–804.
10. Ilea, D.E., Ghita, O., Whelan, P.F.: Evaluation of local orientation for texture classification, in *Proc of the 3rd International Conference on Computer Vision Theory and Applications (VISAPP)*, Funchal, Madeira, Portugal (2008).
11. Kass, M., Witkin, A.: Analyzing oriented patterns, *Computer Vision, Graphics, and Image Processing* **37(3)**, (1987) 362–385.
12. Liu, X., Wang, D.: Texture classification using spectral histograms, *IEEE Transactions on Image Processing* **12(6)**, (2003) 661–670.
13. Manjunath, B.S., Ma, W.Y.: Texture features for browsing and retrieval of image data, *IEEE Transactions on Pattern Analysis and Machine Intelligence* **18(8)**, (1996) 837–842.
14. Materka, A., Strzelecki, M.: Texture analysis methods - A review, Technical Report, University of Lodz, Cost B11 Report, 1998.
15. Mühlich, M., Aach, T.: A theory of multiple orientation estimation, in *Proc of the 9th European Conference on Computer Vision (ECCV)*, Graz, Austria (2006).

16. Ojala, T., Pietikainen, M., Maenpaa, T.: Multiresolution gray-scale and rotation invariant texture classification with local binary patterns, *IEEE Transactions on Pattern Analysis and Machine Intelligence* **24(7)**, (2002) 971–987.
17. Ojala, T., Maenpa, T., Pietikainen, M., Viertola, J., Kyllonen, J., Huovinen, S.: Outex - a new framework for empirical evaluation of texture analysis algorithms, in *Proc. of the 16th International Conference on Pattern Recognition*, vol. 1, Quebec, Canada, (2002) 701–706.
18. Petrou, M., Sevilla, P.G.: *Image Processing: Dealing with Texture*, John Wiley & Sons (2006).
19. Zhou, J., Xin, L., Zhang, D.: Scale-orientation histogram for texture image retrieval, *Pattern Recognition* **36**, (2003) 1061–1063.